Organic & Biomolecular Chemistry

Accepted Manuscript

ROYAL SOCIETY OF CHEMISTRY

www.rsc.org/obc

Journal Name

ARTICLE

Mechanistic insight into the ANRORC-like rearrangement between methylhydrazine and 1,2,4-oxadiazole derivatives.

Received 00th January 20xx,
Accepted 00th January 20xx

DOI: 10.1039/x0xx00000x

www.rsc.org/

Sebastián Gallardo-Fuentes and Renato Contreras

We herein present the first in-deep theoretical study devoted to elucidate the mechanism of the reaction between 1,2,4-oxadiazole derivatives towards methylhydrazine. For this purpose, the reaction between methylhydrazine and some polyfluoroaryl-1,2,4-oxadiazole have been employed as model reactions. The analysis of the potential energy surface (PES) indicates that the most favorable path involves an initial amine attack at the C(2´) site of the aryl moiety to yield an aryl-hydrazine intermediate whose thermodynamic stability appears as the main determinant of the favored reaction path. Next, the cyclization step leading to a spiro intermediate through a favored *5-exo-trig* process appears as rate determining. Additionally, this study highlights the relevance of the torsional strain effects on the favored ANRORC pathway. Finally, both the origins of the substituent effects on the regioselectivity patterns as well as the need of using a large excess of nucleophile to afford the favored ANRORC pathway are discussed.

Introduction

The 1,2,4-oxadiazole derivatives are useful building blocks to obtain a wide number of biologically active molecules, mainly due to its high propensity to rearrange into other more stable nitrogen aromatic heterocycles.[1] In this context, perhaps the most interesting ring transformation process of 1,2,4-oxadiazole derivatives, involves to so-called ANRORC reactions,[2-9] whose mechanism may be divided into the following three key steps: (i) addition of the nucleophile, (ii) ring opening and (iii) ring closure. A sketch of the ANRORC-like rearrangement in 1,2,4-oxadiazole derivatives is depicted in Scheme 1.

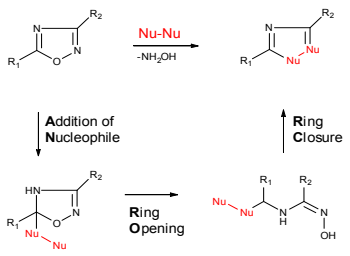

Scheme 1 ANRORC rearrangement of 1,2,4-oxadiazole derivatives with bidentate nucleophiles.

Despite the broad utility of these reactions, only few experimental data have been described in the literature oriented to provide sufficient information about their reaction mechanism.[1] In general, these studies dealt with the substitution patterns at the heterocyclic ring and their effect on the reaction outcome. However, the main factors that determine both, the reactivity and selectivity of these reactions are still an open problem. For instance, the origins of the regioselectivity patterns in these transformations are often been misunderstood and have hitherto been attributed to steric hindrance effects.[4, 9]

Rather recently, Palumbo-Piccionello and co-workers reported the ANRORC-like rearrangement between methyl-hydrazine and some 5-polyfluoroaryl-1,2,4-oxadiazoles.[10] In this transformation, the N(1)-methylindazole regioisomer is the predominant product, even though the relative amount of N(2)-methyl isomer formed is dependent on the substitution pattern at the fluoroaryl moiety. Although some mechanistic aspects have been described for this ANRORC-like transformation, it is not possible at present to provide enough evidence to unambiguously assign the mechanism of this rearrangement. The present study represents a significant step along this line. The article is organized as follows: we first located the most favorable reaction path associated with the formation of the preferred N(1)-methyl isomer; next we focus on the electronic factors that determine the observed regioselectivity. Substituent effects analysis is included in order to describe site activation effects at the electrophilic center of the substrate.

Results and Discussion

Departamento de Química, Facultad de Ciencias, Universidad de Chile, Casilla 653, Santiago, Chile. E-mail: sgallardo@ug.uchile.cl

Electronic Supplementary Information (ESI) available: Computational details, absolute energies, thermochemistry and Cartesian coordinates of all optimized structures. See DOI: 10.1039/x0xx00000x

Reaction Mechanism

In order to better understand the reaction mechanism and the effects of the substituent on the regioselectivity of these reactions, a full exploration of the potential energy surface was performed at the M06-2X/6-31+G(d,p) level of theory.[11, 12] These structures were optimized with the SMD[13] corrections to mimic solvation effects by N,N-dimethylformamide (DMF) used as reaction medium in the experimental study (more details for computational procedure are given in ESI). The first task herein is to obtain the most favorable reaction path associated with the formation of the preferred N(1)-methyl isomer, to assess the origins of the regioselectivity afterwards. For this purpose, the reaction of methylhydrazine with the monofluorinated-1,2,4-oxadiazole **1m** has been employed as model reaction, according to Scheme 2.

In this work, two different mechanisms for the regioselective conversion of **1m** into **2m** were computationally investigated, following the original proposal of Palumbo-Piccionello and co-workers.[10] According to Fig. 1, path 1 involves the initial attack of the NH_2 moiety of the nucleophile to the C(5) site of the heterocyclic ring. This amine attack step has an activation barrier of 17.0 kcal/mol (**TS-1**) and an intermediate lying at 9.0 kcal/mol above reactants (**Int-1**). The subsequent step involves a ring opening process from **Int-1** and passing through the **TS-2** structure. This bond breaking process has an activation barrier of 17.5 kcal/mol and leads to an open chain intermediate **Int-2**. This intermediate can undergo an intramolecular nucleophilic attack with detachment of *o*-fluorine as leaving group from the fluoroaryl moiety to form the desired N(1)-methyl isomer **2m**. The computed activation barrier to reach **TS-3** reveals that this cyclization step is highly disfavored, with a barrier of 22.4 kcal/mol (yielding 34.3 kcal/mol as overall barrier), and therefore qualifying as the rate determining step. It is worth mentioning that the efforts to locate transition structures associated with the leaving group departure were unsuccessful, presumably because this step is extremely fast. This hypothesis is reinforced by an IRC analysis, where it is possible to note a reaction path that resembles a two-step no intermediate mechanism[14] for this cyclization stage. Fig. 2 displays the transition state structures for the ANRORC rearrangement via the proposed path 1.

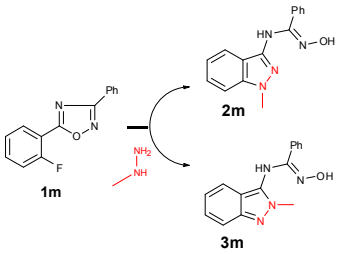

Scheme 2 Regioselective ANRORC rearrangement of methylhydrazine with 5-(2-fluorophenyl)-3-phenyl-1,2,4-oxadiazole used as model reaction.

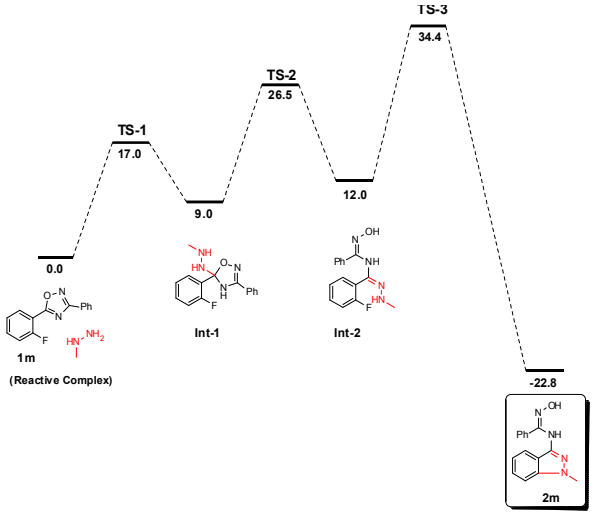

Fig. 1 Relative free energies (in kcal/mol) among the different species involved in path 1 for the ANRORC rearrangement of the title reactions.

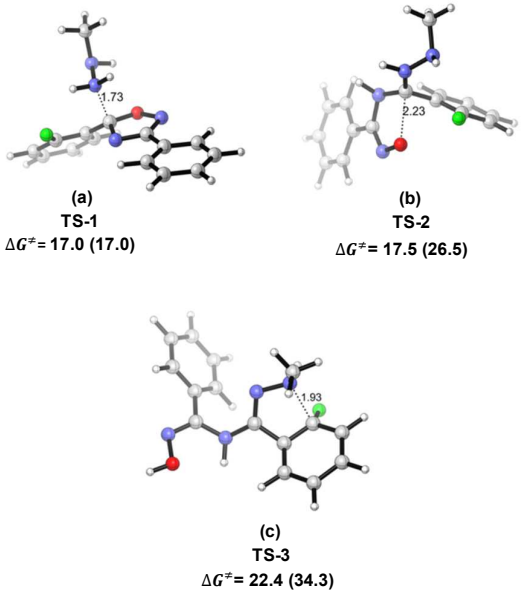

Fig. 2 Transition state structures for the ANRORC-like rearrangement of the title reaction via path 1: (a) nucleophilic attack, (b) ring opening and (c) ring closure steps. Free energies are given in kcal/mol. In parenthesis are given the overall barriers.

The second alternative considered is path 2, which is depicted in Fig. 3. It begins with the well-known S_NAr reaction.[15-17] Here, the first step is the formation of the σ-complex that occurs after the nucleophilic attack of the NHMe end of the methylhydrazine to the fluoroaryl moiety. This amine attack step proceeds via **TS-4** with a barrier of 15.4 kcal/mol and leads to the zwitterionic σ-complex **Int-3** located to 13.5 kcal/mol above reactants (see Fig. 3).

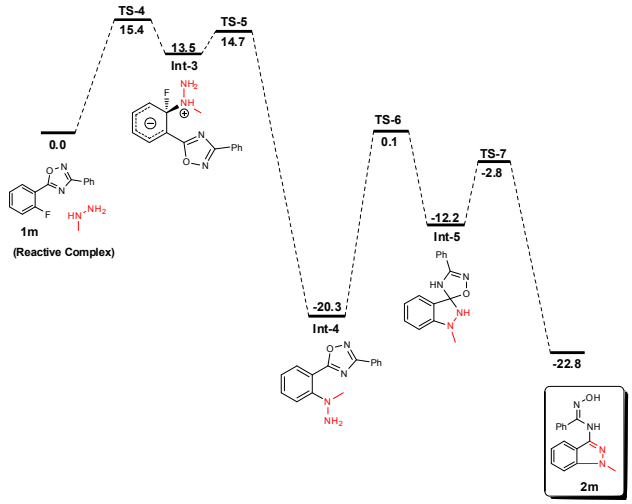

Fig. 3 Relative free energies (in kcal/mol) among the different species involved in path 2 for the ANRORC-like rearrangement of the title reactions.

The second step involves the departure of the leaving group, which is predicted to be a facile process with an activation barrier of only 1.2 kcal/mol, leading to the thermodynamically stable arylhydrazine intermediate **Int-4**. Figs. 4a and 4b show the S_NAr transition structures **TS-4** and **TS-5** respectively. From these structures, it is possible to note the key role of 1,2,4-oxadiazole moiety in this mechanism. First, by acting as an electro-withdrawing group capable of activating the ipso position of the aryl moiety and secondly, allowing the formation of an intramolecular hydrogen-bond (HB) interaction which has been proposed to play a key role in the S_NAr mechanism.[18-20] This process is followed by an intramolecular nucleophilic attack of the β nitrogen of the intermediate **Int-4** on the C(5) atom of the oxadiazole group to give the spiro intermediate **Int-5**. This step takes place via a favored *5-exo-trig*[21] transition structure **TS-6** and shows a barrier of about 20.4 kcal/mol. The high energy barrier obtained for this step is attributed to two main factors, arising from an aryl-oxadiazole distortion at the TS structure, namely: (i) the loss of a resonance stabilization as response to the lack of co-planarity between the aryl and oxadiazole moiety and (ii) the torsional effects imposed by the aryl tether that resembles an 1,3-allylic strain,[22] as shown in Fig. 4c. Indeed, the intermolecular nucleophilic attack of NH_2 moiety at C(5) atom of the azole ring (via **TS-1**) lies 3.4 kcal/mol lower than the corresponding intramolecular amine attack that take place via **TS-6** transition structure. In the last step the spiro intermediate can undergo a ring-opening process to yield the desired N(1)-methyl isomer. For this ring cleavage process, two scenarios are possible. The first one involves a pathway that start at the proposed **Int-5** structure and proceeds via **TS-7** with an activation barrier of about 9.4 kcal/mol, (see Fig. 4d). On the other hand, a second scenario implies a ring opening process that take place via the zwitterionic structure **TS-7zw** (Fig. 4e). Nevertheless, our calculations indicate that this bond-breaking process is highly disfavored with a transition structure (**TS-7zw**) lying at 27.2 kcal/mol above the most favored **TS-7** structure. This difference in the reactivity patterns, which may at first glance be attributed to a process with an early transition state,[23-25] can be understood as a response to stereo-electronic effects. In this context, the C-O bond-breaking process is better assisted by the unshared electron pair located at the NH functionality of indazole fragment instead of the electron pair delocalized at the 1,2,4-oxadiazole moiety (see Figs. 4d and 4e).

On the other hand, because of their key role in the ring opening step, the formation of intermediate **Int-5** from **Int-5zw** via a proton transfer mechanism has also been explored in detail (see Fig. 5). In order to test this prognosis, two competitive reaction pathways were further considered. The first attempt was the evaluation of a plausible intramolecular proton transfer between the NH_2 functionality of indazole fragment towards N4 site of oxadiazole moiety via **TS-PT1** transition structure (see Fig. 5).

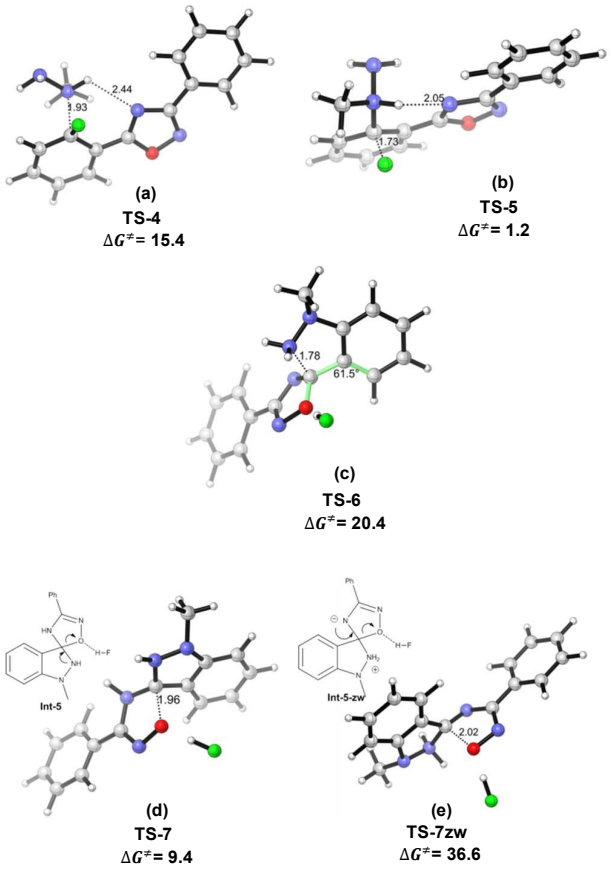

Fig. 4 M06-2X/6-31+G(d,p) transition state structures for the ANRORC rearrangement of the title reactions. (a) nucleophilic attack, (b) leaving group departure step, (c) cyclization stage via favored 5-*exo-trig* process, and intramolecular ring opening step transition state via a neutral intermediate (d) of through a zwitterionic intermediate (f). Free energies are given in kcal/mol. Distances in Å.

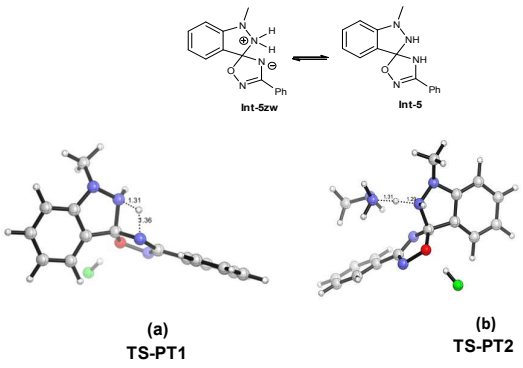

Fig. 5 Proton transfer step to give the key intermediate **Int-5**

However, our results show that this intramolecular proton shift is highly disfavored; with an overall activation barrier of 45.6 kcal/mol (relative to **Int-4**). A second possibility involves a nucleophile-assisted proton transfer between the same fragments, but this time assisted by a second nucleophile molecule. This proton shift catalyzed by a second nucleophile molecule takes place via **TS-PT2** transition structure in Fig. 5. This process was calculated to have a barrier of 2.4 kcal/mol. It must be stressed that this result is consistent with the experimental observation where the use of a large excess of nucleophile plays a key role on the reaction outcome.

During the review process of this article, a referee called our attention to consider exploring an alternative mechanism which involves the formation of a ketenimine intermediate. However, our calculations reveal that this proposed mechanism is highly disfavored: the ketenimine intermediate lies 46.8 kcal/mol ($\Delta\Delta G^{\neq}$) higher than the corresponding Meisenheimer-like intermediate (**Int-3**) described herein. These results confirm that the S_NAr pathway is the dominant mechanism for the initial nucleophilic attack step of the title reactions.

Finally, by comparing the PES for both proposed mechanism (Figs. 1 and 3), it is possible to note that the reaction path that begins with the initial attack of NHMe end of the nucleophile at the 2´-position of the fluoroaryl moiety appears as the most favorable path. Nevertheless, it is interesting to note that the energetically lower path that proceeds via *5-exo-trig* cyclization as the rate determining step **(TS-6)** is only 2.0 kcal/mol lower in free energy than the corresponding rate determining **TS-3** structure. According to these results, we suggest that the prevalence of this reaction pathway is controlled by the preferential formation of the **Int-4** intermediate, whose thermodynamic stability with respect to **Int-1** appears as the driving force for this mechanism.

Substituent effects on the regioselectivity patterns

Having established the most favored path, we now evaluate the origins of the regioselective formation of N(1)-methyl isomer instead of the N(2)-methyl isomer. According to the results discussed above, the rate determining step involves an intramolecular process that begins at the aryl-hydrazine intermediate **Int-4** region of the PES. Because the intramolecular nucleophilic attack is a first order process, the ratio of regioisomers population can be expressed as follows:

$$\frac{[P_1]}{[P_2]} = \frac{[Int4_{(N1)}]}{[Int4_{(N2)}]} \times \frac{e^{-(k_{im2}t)}}{e^{-(k_{im1}t)}} \qquad (1);$$

In this equation $[P_1]$ and $[P_2]$ are the concentrations of N(1)-methyl and N(2)-methylindazole isomers (the reaction products), whereas the [Int-4(N1)]/[Int-4(N2)] ratio refers to the relative populations of aryl-hydrazine intermediates. This ratio can be readily obtained by using the Curtin-Hammett principle.[26] The exponential factor assesses the contribution of intramolecular process to the observed regioselectivity. In this context, we envisage that the regioselectivity patterns may be ascribed to the preferential formation of the N(1)-methyl aryl-hydrazine intermediate (Int-4(N1) in equation 1).

The computed activation barrier for the rate determining transition structure that leads to N(2)-methylindazole isomer as product is predicted to be only 0.3 kcal/mol lower than the corresponding **TS-4** (see ESI for more details). Furthermore, the $\Delta\Delta G^{\neq}$ values calculated for the regioselective addition of methylhydrazine at the C(2´) position of aryl moiety (6.4 kcal/mol) is in good agreement with the experimental data obtained for the model reaction, where the exclusive formation of N(1)-methyl isomer is reported in high yield. This result not only confirms the hypothesis previously advanced, but also highlights the relevance of torsional strain effects[27] on the rate determining step, that are clearly more important than the electronic effects.

On the other hand, the enhanced amount of N(2)-methylindazole is related to the substitution pattern at the aryl moiety. In this context, when the 5-(2-fluorophenyl) substituent on the 1,2,4-oxadiazole moiety is replaced by the 5-(2,3-difluoro-4-methoxyphenyl) group the experimental selectivity is 19.3:1. On the other hand, in the presence of a polyfluorinated group, namely 5-(2,3,5,6-tetrafluoro-4-methoxyphenyl) the yield of N(2)-methyl isomer is increased with a regioselectivity of 4.3:1 (see Scheme 3). Therefore, we located the transition structures for the attack of methylhydrazine on C(2´) site (analogous to **TS-4**) for fluorinated substituted 1,2,4-oxadiazol, namely **TS-2a**, **TS-2b**, **TS-3a** and **TS-3b** in order to assess the role of substitution patterns on the regioselectivity. For this purpose, we compared their observed selectivities with the predicted $\Delta\Delta G^{\neq}$ values. This substituted transition structures are shown in Fig. 6.

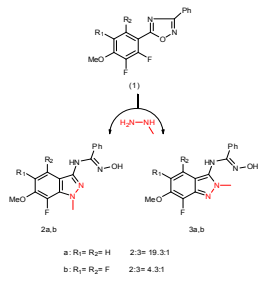

Scheme 3 Substituent effects on the regioselectivity patterns.

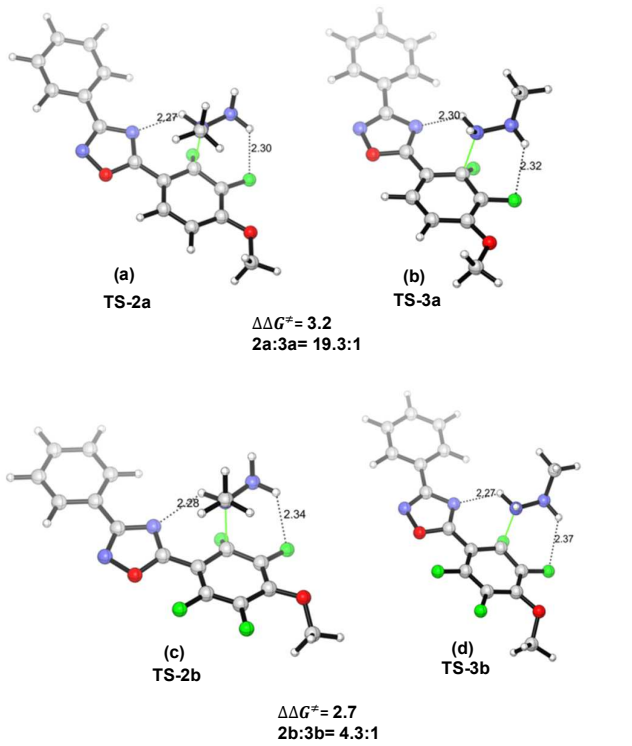

Fig. 6 Relative free energies (in kcal/mol) of the regioisomeric transition state for the addition of methylhydrazine towards 1,2,4-oxadiazole derivatives. Distances are given in Å.

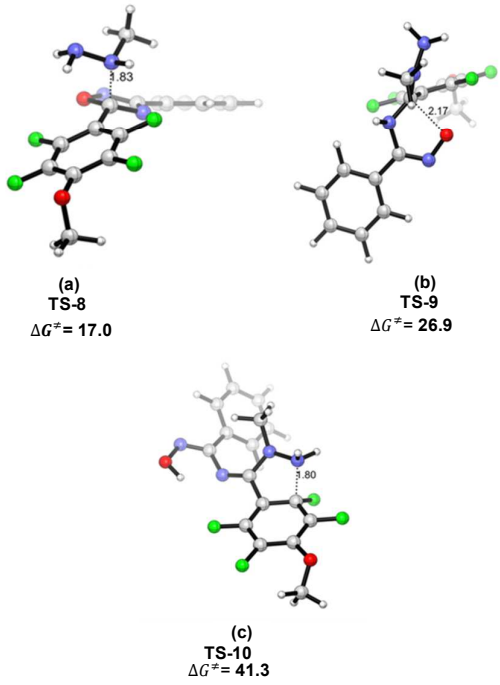

Fig. 7 M06-2X/6-31+G(d,p) optimized transition state structures for the feasibility of the formation of the N(2)-methyl isomer along the probable competitive path involving (a) nucleophilic attack of the NHMe group on C(5) site; (b) ring opening and (c) ring closure steps. Free energies are given in kcal/mol. Distances are given in Å.

As shown in Fig. 6, the presence of an *o*-fluorine substituent at the fluoroaryl moiety capable of engaging into an intramolecular HB interaction with the nucleophile facilitates the nucleophilic attack of NH_2 moiety towards the oxadiazole compounds **1a** with respect to the model substrate **1m**. This response can be explained as a site activation effect that elicits an enhancing of the nucleophilicity of the attacking site of the alpha-nucleophile.[28] In round words; in the absence of this interaction, the nucleophilic attack (and the regioselectivity patterns) is governed by the difference between the intrinsic nucleophilic nature of both NH_2 and NHMe sites,[29, 30] whereas when a site activation mechanism is feasible, the activating effects at the reaction centre seems to be more important for the regioselectivity of the reaction. On the other hand, the polarization effects induced by fluorine groups at the C(5´) and C(6´) sites cause a lowering in the selectivity patterns (see for instance transition structures **TS-2b** and **TS-3b** in Fig. 6). Therefore, the calculated selectivity of N(1)-methyl isomer for both mono-fluorinated and polyfluorinated compounds agrees well with the higher regioselectivity observed for this isomer.

On the other hand, we evaluated the feasibility of forming the N(2) methyl isomer by means of a competitive reaction path, that involve the initial amine attack of the NHMe end of the methylhydrazine nucleophile on the C(5) site of oxadiazole moiety. The transition structures involved in this path are depicted in Fig. 7.

Finally, it must be noted that the **TS** structure for the nucleophilic attack step of NHMe end of methylhydrazine on the C(5) site of oxadiazole functionality lies 0.3 kcal/mol higher than the corresponding amine attack on C(2´) site of fluoroaryl moiety, suggesting that both amine attack mechanisms can be competitive. However, even in presence of electro-withdrawing groups at the fluoroaryl moiety, the intramolecular S_NAr process is still highly disfavored, with an overall activation barrier of 41.3 kcal/mol. Thereby, these results discard the role of the initial nucleophilic attack step on the reaction outcome as it was proposed elsewhere.

Conclusions

Herein we have presented an in-depth theoretical study on the ANRORC-like rearrangement of methylhydrazine with 1,2,4-oxadiazole derivatives. This first computational study on the mechanism of the title reaction provides a deeper understanding on the origins of reactivity and regioselectivity of these processes. Thus, the main results obtained in this study are summarized as follows: (i) the most favourable path involve an initial amine attack onto the C(2´) site of the aryl moiety to yield an aryl hydrazine intermediate whose thermodynamic stability appears as the driving force for this ANRORC-like path, (ii) the cyclization step to yield a spiro intermediate appears as the rate determining step. This response is due to the torsional strain effects presents at the

transition state where the reacting atoms are arranged in a 5-exo-trig mode and the aryl tether is settled in a 1,3-allylic-like fashion, (iii) the nucleophilic-assisted proton transfer is a crucial step for the achievement of desired methylindazole as reaction product, (iv) the regioselectivity patterns are determined by site activation effects brought about by an intramolecular HB interaction at the transition state. Thus, in the absence of this interaction, the regioselectivity patterns are governed by the difference between the intrinsic nucleophilic nature of both NH_2 and NHMe ends. These conclusions are in good agreement with the experimental data reported by Palumbo-Piccionello and co-workers.

Acknowledgements

This work was supported by Project ICM: RC-130006-CILIS, granted by Fondo de Innovación para la Competitividad del Ministerio de Economía, Fomento y Turismo, Chile and Conicyt grant 21120876.

Notes and references

1 A. Pace and P. Pierro, *Org. Biomol. Chem.*, 2009, **7**, 4337-4348.
2 H. C. Van der Plas, *Acc. Chem. Res.*, 1978, **11**, 462-468.
3 S. Buscemi, A. Pace, I. Pibiri, N. Vivona, Camilla Z. Lanza and D. Spinelli, *Eur. J. Org. Chem.*, 2004, **2004**, 974-980.
4 S. Buscemi, A. Pace, A. P. Piccionello, I. Pibiri, N. Vivona, G. Giorgi, A. Mazzanti and D. Spinelli, *J. Org. Chem.*, 2006, **71**, 8106-8113.
5 A. Palumbo Piccionello, A. Pace, I. Pibiri, S. Buscemi and N. Vivona, *Tetrahedron*, 2006, **62**, 8792-8797.
6 A. P. Piccionello, A. Pace, S. Buscemi, N. Vivona and G. Giorgi, *Tetrahedron Lett.*, 2009, **50**, 1472-1474.
7 A. Palumbo Piccionello, A. Guarcello, S. Buscemi, N. Vivona and A. Pace, *J. Org. Chem.*, 2010, **75**, 8724-8727.
8 A. Palumbo Piccionello, A. Pace and S. Buscemi, *Org. Lett.*, 2011, **13**, 4749-4751.
9 S. Buscemi, A. Pace, I. Pibiri, N. Vivona and D. Spinelli, *J. Org. Chem.*, 2003, **68**, 605-608.
10 A. Palumbo Piccionello, A. Pace, P. Pierro, I. Pibiri, S. Buscemi and N. Vivona, *Tetrahedron*, 2009, **65**, 119-127.
11 Y. Zhao and D. Truhlar, *Theor Chem Account*, 2008, **120**, 215-241.
12 Y. Zhao and D. G. Truhlar, *Acc. Chem. Res.*, 2008, **41**, 157-167.
13 A. V. Marenich, C. J. Cramer and D. G. Truhlar, *J. Phys. Chem. B*, 2009, **113**, 6378-6396.
14 D. H. Ess, S. E. Wheeler, R. G. Iafe, L. Xu, N. Çelebi-Ölçüm and K. N. Houk, *Angew. Chem., Int. Ed.*, 2008, **47**, 7592-7601.
15 J. F. Bunnett and R. E. Zahler, *Chem. Rev.*, 1951, **49**, 273-412.
16 P. S. Kalsi, *Organic Reactions And Their Mechanisms*, New Age International (P) Limited, 2009.
17 F. Terrier, *Modern Nucleophilic Aromatic Substitution*, Wiley, 2013.
18 N. Chéron, L. El Kaïm, L. Grimaud and P. Fleurat-Lessard, *Chem. Eur. J*, 2011, **17**, 14929-14934.
19 R. Ormazabal-Toledo, R. Contreras, R. A. Tapia and P. R. Campodonico, *Org. Biomol. Chem.*, 2013, **11**, 2302-2309.
20 R. Ormazábal-Toledo, R. Contreras and P. R. Campodónico, *J. Org. Chem.*, 2013, **78**, 1091-1097.
21 J. E. Baldwin, *J. Chem. Soc., Chem. Commun.*, 1976, 734-736.
22 R. W. Hoffmann, *Chem. Rev.*, 1989, **89**, 1841-1860.
23 G. S. Hammond, *J. Am. Chem. Soc.*, 1955, **77**, 334-338.
24 T. H. Lowry and K. S. Richardson, *Mechanism and theory in organic chemistry*, Harper & Row, 1987.
25 A. Pross, *Theoretical and Physical Principles of Organic Reactivity*, Wiley, 1995.
26 J. I. Seeman, *Chem. Rev.*, 1983, **83**, 83-134.
27 K. B. Wiberg, *Angew. Chem., Int. Ed.*, 1986, **25**, 312-322.
28 S. Gallardo-Fuentes, R. A. Tapia, R. Contreras and P. R. Campodonico, *RSC Advances*, 2014, **4**, 30638-30643.
29 T. A. Nigst, A. Antipova and H. Mayr, *J. Org. Chem.*, 2012, **77**, 8142-8155.
30 T. A. Nigst, J. Ammer and H. Mayr, *Angew. Chem., Int. Ed.*, 2012, **51**, 1353-1356.